This article has been accepted for inclusion in a future issue of this journal. Content is final as presented, with the exception of pagination.

Hilbert Transform Design Based on Fractional Derivatives and Swarm Optimization

Anil Kumar, *Member, IEEE*, Nikhil Agrawal, *Student Member, IEEE*, Ila Sharma, *Student Member, IEEE*, Seungchan Lee, and Heung-No Lee, *Senior Member, IEEE*

***Abstract*—This paper presents a new efficient method for implementing the Hilbert transform using an all-pass filter, based on fractional derivatives (FDs) and swarm optimization. In the proposed method, the squared error difference between the desired and designed responses of a filter is minimized. FDs are introduced to achieve higher accuracy at the reference frequency (ω_0), which helps to reduce the overall phase error. In this paper, two approaches are used for finding the appropriate values of the FDs and reference frequencies. In the first approach, these values are estimated from a series of experiments, which require more computation time but produce less accurate results. These experiments, however, justify the behavior of the error function, with respect to the FD and ω_0, as a multimodal and nonconvex problem. In the second approach, a variant of the swarm-intelligence-based multimodal search space technique, known as the constraint-factor particle swarm optimization, is exploited for finding the suitable values for the FD and ω_0. The performance of the proposed FD-based method is measured in terms of fidelity aspects, such as the maximum phase error, total squared phase error, maximum group delay error, and total squared group delay error. The FD-based approach is found to reduce the total phase error by 57% by exploiting only two FDs.**

***Index Terms*—Evolutionary technique (ET), fractional derivative (FD), Hilbert transform (HT), particle swarm optimization (PSO).**

I. Introduction

HILBERT transform (HT) is a very important transform in signal processing. It can be used to represent a narrow-band signal in terms of its frequency-domain amplitude at a frequency-modulation point. HT is useful in many applications such as latency analysis in neurophysiological signals [1], fault classification in electrical systems, data compression in communication, and as an data analysis tool [2], [3]. Research on efficient HT design methods has been progressing over the last three decades. In the early stages of research, several works used infinite impulse response (IIR) filters, which satisfied the magnitude and phase specifications simultaneously [4]–[8]. In these techniques, the design problem was formulated as a minimization of the mean squared error between the desired and designed responses, and the solution was obtained by solving a set of linear equations [5]–[8]. Squared error-based methods usually produced a matrix, which was symmetric and positive definite, and the solutions of such problems were computed by either evaluating the eigen vector (EV) corresponding to the least value of the eigen value or multiplying the matrix inverse with the multiplicand. The EV approach was computationally complex, whereas the second approach had $o(n^3)$ complexity. However, this complexity could be reduced to $o(n^2)$ using the Cholesky decomposition or split Levinson algorithms [9]. Liu [1] and Kidambi [7] used a Toeplitz-plus-Hankel matrix to solve a set of linear equations. For reducing the computational complexity further, Su *et al.* [9] proposed a closed-form method for the design of the HT. Literature review on the implementation of HT using all-pass filters (APFs) has corroborated that several methods have been proposed [4]–[8]. However, an APF with smaller number of filter taps and higher accuracy in terms of the degree of approximation, which can produce a desired response at a certain reference frequency point, has not been considered yet for the efficient design of an HT.

Recently, fractional derivatives (FDs) have been used in several engineering problems, such as fractional system identification, edge detection in image processing, electrocardiogram signal R-peak detection, and numerous other engineering applications, owing to their ease of realization and higher efficiency compared to integral-order derivatives [10]–[15]. Several researchers have used FDs for digital filter design [13]–[15]. In these techniques, the determination of optimal orders of FDs was computationally expensive, and the work involved increases with the increase in the order of FD. A possible solution for this problem is to use evolutionary techniques (ETs) for filter-bank design, which is explained in [15]. However, a mechanism to tune the suitable values of the reference frequency in the region of interest, where these FDs are being evaluated, has not been established yet.

Manuscript received September 13, 2018; revised September 26, 2018; accepted October 8, 2018. This work was supported by the National Research Foundation of Korea (NRF) funded by the Korean Government (MSIP) under Grant NRF-2018R1A2A1A19018665. This paper was recommended by Associate Editor Q. Zhang. *(Corresponding author: Heung-No Lee.)*

A. Kumar is with the Department of Electronics and Communication Engineering, PDPM Indian Institute of Information Technology, Design and Manufacturing Jabalpur, Jabalpur 482005, India, and also with the School of Electrical Engineering and Computer Science, Gwangju Institute of Science and Technology, Gwangju 61005, South Korea (e-mail: anilkdee@gmail.com).

N. Agrawal and I. Sharma are with the Department of Electronics and Communication Engineering, PDPM Indian Institute of Information Technology, Design and Manufacturing Jabalpur, Jabalpur 482005, India (e-mail: nikhil.agrawal@iiitdmj.ac.in; ilasharma23@gmail.com).

S. Lee and H.-N. Lee are with the School of Electrical Engineering and Computer Science, Gwangju Institute of Science and Technology, Gwangju 61005, South Korea (e-mail: heungno@gist.ac.kr; seungchan@gist.ac.kr).

Color versions of one or more of the figures in this paper are available online at http://ieeexplore.ieee.org.

Digital Object Identifier 10.1109/TCYB.2018.2875540

2168-2267 © 2018 IEEE. Personal use is permitted, but republication/redistribution requires IEEE permission.
See http://www.ieee.org/publications_standards/publications/rights/index.html for more information.

This article has been accepted for inclusion in a future issue of this journal. Content is final as presented, with the exception of pagination.

This paper explores a new design technique for the HT, which uses APFs with a high approximation of the desired phase response, based on optimal values of FDs and suitable values of reference points in the region of interests. The Lagrange multiplier method is used to solve the formulated constrained design problem. A variant of particle swarm optimization (PSO), known as constraint-factor PSO (CF-PSO) is used for determining the suitable values of the FDs and reference frequency points.

The remainder of this paper is organized as follows. Section II provides the brief description on PSO variant and its topology. Section III provides the details of HT design using an IIR-APF. Sections IV and V describe the proposed approach using FD for HT design. Section VI demonstrates the performance of the proposed method and improvement with earlier state-of-art techniques. Finally, the conclusive remarks are mentioned in Section VII.

II. Overview of PSO

PSO is a swarm-intelligence-based algorithm, inspired by the communication behaviors of birds and insects, schooling of fish, etc. [16]. In the past few decades, exhaustive research has been conducted on the application of PSO for solving nondifferentiable, multiobjective, and nonlinear problems [16]–[18]. The search space in PSO is a matrix that consists of a solution vector, which is updated as [16]

$$[\boldsymbol{U}]^{k+1} = [\boldsymbol{U}]^{k} + [\boldsymbol{V}]^{k+1} \tag{1}$$

where $[\boldsymbol{V}]^{k+1}$ is the current velocity matrix and $\boldsymbol{U}$ is the search space matrix. The sizes of both matrixes are $R \times T$, where R is the number of solution vectors, T is the dimension of solution vector, and k+1 is the current iteration. $[\boldsymbol{V}]^{k+1}$ is computed as [16]

$$[\boldsymbol{V}]^{k+1} = \chi \left\{ \begin{array}{l} w \cdot [\boldsymbol{V}]^{k} + c_1^k \cdot \boldsymbol{\phi}_1 \cdot \left([\boldsymbol{PB}]^k - [\boldsymbol{U}]^k\right) \\ + c_2^k \cdot \phi_2 \cdot \left([\boldsymbol{GB}]^k - [\boldsymbol{U}]^k\right) \end{array} \right\}. \tag{2}$$

In (2), $\boldsymbol{PB}$ is the local best solution matrix, $\boldsymbol{GB}$ is the current global best solution vector, $\boldsymbol{\varphi}_1$ and $\boldsymbol{\varphi}_2$ are uniformly distributed random numbers in the interval (0, 1], cognitive (c_1) and social (c_2) are the acceleration coefficients, w is the inertia of weight, and χ is a constraint factor. Modification in the values of control parameters, such as w or c_1 and c_2 results in several variants of PSO, as described in [16].

Many researchers have attempted to discover new aspects in PSO, to avoid phenomena, such as trapping in local minima and premature convergence and to accomplish the efficient exploitation with deeper exploration, which has resulted in several variants of PSO [16]. The principle mechanism of all variants of PSO is the same and is summarized as follows.

1) Form the initial search space (possible solutions).
2) Evaluate the fitness function for each individual solution vector of the search space.
3) Sort out the solution vector with the best fitness, termed as *Global best.*
4) Update the initially formed search space and find solutions, which have improved their fitness, and consider them instead of old solutions with less fitness.
5) Find the best fitness formed from recently updated solutions, and check if it is better than the current best solution; then, update *Global best.*

Among the variants of PSO, CF-PSO is more stable, owing to χ, which aids in keeping a bound on the exploration and exploitation [16]. Various neighborhood topologies have also been proposed for PSO, such as the global PSO (Gbest) and local PSO (Lbest). Lbest is further classified as von Neumann, star, ring, and pyramid [19]. In this paper, the Gbest structure has been exploited because of its fastest convergence speed [19]. The search mechanism in PSO is simpler than that of other techniques, such as differential evolution, genetic algorithm, improved JADE, LSHADE, etc. [20], [21].

III. All-Pass Filter Design

Several design methodologies have been proposed for designing the HTs using all-pass IIR filters, based on either the least-squares (LSs) approximation or minimax approximation criteria [7]. The frequency response of an all-pass transfer function is expressed as [4]

$$H_o(z) = z^{-N} \frac{\sum_{n=0}^{N} b(n) z^{n}}{\sum_{n=0}^{N} b(n) z^{-n}} = e^{-jN\omega} \frac{\sum_{n=0}^{N} b(n) e^{jn\omega}}{\sum_{n=0}^{N} b(n) e^{-jn\omega}} \tag{3}$$

$$H_o\left(e^{j\omega}\right) = e^{-jN\omega} \frac{1 + \sum_{n=1}^{N} b(n)\cos(n\omega) + j\sum_{n=1}^{N} b(n)\sin(n\omega)}{1 + \sum_{n=1}^{N} b(n)\cos(n\omega) - j\sum_{n=1}^{N} b(n)\sin(n\omega)} \tag{4}$$

and

$$H_o\left(e^{j\omega}\right) = e^{j\varphi(\omega)}. \tag{5}$$

In (3) and (4), $b(n)$ is a real-valued integer and N is the total number of filter taps. The phase response of the denominator polynomial ($\sum_{n=0}^{N} b(n)e^{-jn\omega}$) is

$$\varphi(\omega) = -N\omega + 2 \times \tan^{-1}\left(\frac{\sum_{n=1}^{N} b(n)\sin(n\omega)}{1 + \sum_{n=1}^{N} b(n)\cos(n\omega)}\right). \tag{6}$$

The error difference between the desired $\{\varphi_d(\omega)\}$ and designed phase is computed as

$$e_o(\omega) = \varphi_d(\omega) + N\omega - 2 \times \tan^{-1}\left(\frac{\sum_{n=1}^{N} b(n)\sin(n\omega)}{1 + \sum_{n=1}^{N} b(n)\cos(n\omega)}\right). \tag{7}$$

For designing a Hilbert transformer, $\varphi_d(\omega)$ of an APF is given as [4], [7]

$$\varphi_d(\omega) = -N\omega - \frac{\pi}{2}. \tag{8}$$

It is evident from (7) that the minimization of phase error is a multimodal complex problem because of the trigonometric function, and can be simplified by setting $e_o(\omega) = 0$, as

$$\tan\left(\frac{\varphi_d(\omega) + N\omega}{2}\right) = \frac{\sum_{n=1}^{N} b(n)\sin(n\omega)}{1 + \sum_{n=1}^{N} b(n)\cos(n\omega)} \tag{9}$$

and further refined to a more compact form as

$$\frac{\sin\left[-\pi/4\right]}{\cos\left[-\pi/4\right]} = \frac{\boldsymbol{b}^{\mathrm{T}} \cdot \boldsymbol{s}(\omega)}{1 + \boldsymbol{b}^{\mathrm{T}} \cdot \boldsymbol{c}(\omega)}. \tag{10}$$

This article has been accepted for inclusion in a future issue of this journal. Content is final as presented, with the exception of pagination.

In the above equation, $\boldsymbol{b}$, $\boldsymbol{s}(\omega)$, and $\boldsymbol{c}(\omega)$ are the vectors, defined as

$$\boldsymbol{b} = [b(1)b(2)\ldots b(N)]^{\mathrm{T}} \tag{11}$$

$$\boldsymbol{s}(\omega) = [\sin(\omega)\sin(2\omega)\ldots\sin(N\omega)]^{\mathrm{T}} \tag{12}$$

and

$$\boldsymbol{c}(\omega) = [\cos(\omega)\cos(2\omega)\ldots\cos(N\omega)]^{\mathrm{T}}. \tag{13}$$

On rearranging (10), the required design constraint for obtaining a desired phase response is given as

$$\boldsymbol{b}^{\mathrm{T}}\left\{\sin\left[{}^{-\pi}\!/_4\right]\boldsymbol{c}(\omega) - \cos\left[{}^{-\pi}\!/_4\right]\boldsymbol{s}(\omega)\right\} = -\sin\left[{}^{-\pi}\!/_4\right] \tag{14}$$

or

$$\boldsymbol{b}^{\mathrm{T}}\boldsymbol{S}_o(\omega) = B(\omega) = -\sin\left[{}^{-\pi}\!/_4\right] \tag{15}$$

where

$$\begin{aligned}\boldsymbol{S}_o(\omega) &= \sin\left[{}^{-\pi}\!/_4\right]\boldsymbol{c}(\omega) - \cos\left[{}^{-\pi}\!/_4\right]\boldsymbol{s}(\omega)\\ &= \sin\left[{}^{-\pi}\!/_4 - n\omega\right], \quad 1 \le n \le N.\end{aligned} \tag{16}$$

A possible solution for the above problem is obtained by solving a set of equations formed by constructing an LS error function, defined as

$$E_o(\boldsymbol{b}) = \int_{\omega_1}^{\omega_2}\left\{\boldsymbol{b}^{\mathrm{T}}\boldsymbol{S}_o(\omega) + \sin\left[{}^{-\pi}\!/_4\right]\right\}^2 d\omega \tag{17}$$

where ω_1 is the lower and ω_2 is the upper frequency limit for the region of interest. Now, by expanding and partially differentiating (17) with respect to $\boldsymbol{b}$, we obtain

$$\frac{\partial E_o(\boldsymbol{b})}{\partial \boldsymbol{b}} = \frac{\partial\left\{\begin{array}{l}\boldsymbol{b}^{\mathrm{T}}\left(\int_{\omega_1}^{\omega_2}\left[\boldsymbol{S}_o(\omega)\boldsymbol{S}_o^{\mathrm{T}}(\omega)\right]d\omega\right)\boldsymbol{b}\\ +\,2\boldsymbol{b}^{\mathrm{T}}\left(\int_{\omega_1}^{\omega_2}\left[\sin\left[{}^{-\pi}\!/_4\right]\boldsymbol{S}_o(\omega)\right]d\omega\right)\\ +\int_{\omega_1}^{\omega_2}\left(\sin^2\left[{}^{-\pi}\!/_4\right]\right)d\omega\end{array}\right\}}{\partial \boldsymbol{b}}. \tag{18}$$

By setting ${}^{\partial E_o(\boldsymbol{b})}\!/_{\partial \boldsymbol{b}} = 0$, the required filter coefficient is obtained by solving $\boldsymbol{b}_{\mathrm{opt}} = \boldsymbol{Q}^{-1}\cdot\boldsymbol{P}$, where

$$\boldsymbol{Q} = \int_{\omega_1}^{\omega_2}\left[\boldsymbol{S}_o(\omega)\boldsymbol{S}_o^{\mathrm{T}}(\omega)\right]d\omega \tag{19}$$

and

$$\boldsymbol{P} = \int_{\omega_1}^{\omega_2}\left[\sin\left[{}^{-\pi}\!/_4\right]\boldsymbol{S}_o(\omega)\right]d\omega. \tag{20}$$

In (19), $\boldsymbol{Q}$ is a real, positive-definite, and symmetric matrix; thus, a unique solution is guaranteed. In [7], $\boldsymbol{Q}$ is simplified and represented by the sum of a Toeplitz matrix and a Hankel matrix. However, in this paper, it is further reduced to a single term, obtained by the multiplication of vector $\boldsymbol{S}_o(\omega)$ with its transpose. In order to achieve a high degree of similarity between the desired phase response and the designed phase response at the prescribed frequency point ω_0, the following constraints are imposed:

$$B(\omega_o) = \sin\left({}^{\pi}\!/_4\right) \tag{21}$$

and

$$D^{v}B(\omega)|_{\omega=\omega_o} = 0 \tag{22}$$

where $B(\omega) = \boldsymbol{b}^{\mathrm{T}}\boldsymbol{S}_o(\omega)$.

IV. Problem Formulation Using FDs

FDs have been found to function as performance boosters in several signal-processing applications [11]–[15]. Three of the most prominent definitions of FDs are the Riemann–Liouville, Grünwald–Letnikov (GL), and Caputo definitions [13]. Among these definitions, the GL derivative method is the most commonly used method in signal-processing applications, owing to its simplicity and low complexity [15]. In this paper, the GL derivative method is used to design a Hilbert transformer using an APF.

Using the GL definition [13], (22) can be reduced to

$$\begin{aligned}D^{v}B(\omega) &= \frac{d^{v}\left(\sum_{n=1}^{N} b(n)\cdot\sin\left({}^{-\pi}\!/_4 - n\omega\right)\right)}{d\omega^{v}}\\ &= \sum_{n=1}^{N} b(n)\cdot(n)^{v} - \sin\left({}^{\pi}\!/_4 + n\omega + \frac{\pi v}{2}\right)\\ &= \boldsymbol{b}^{\mathrm{T}}\boldsymbol{C}(\omega, v).\end{aligned} \tag{23}$$

$\boldsymbol{C}(\omega, v)$ is given by

$$\boldsymbol{C}(\omega, v) = \begin{bmatrix}-(1)^{v}\cdot\sin\left(\omega + \frac{\pi}{4} + \frac{\pi v}{2}\right)\\ -(2)^{v}\cdot\sin\left(2\omega + \frac{\pi}{4} + \frac{\pi v}{2}\right)\\ \vdots\\ -(N)^{v}\cdot\sin\left(N\omega + \frac{\pi}{4} + \frac{\pi v}{2}\right)\end{bmatrix}. \tag{24}$$

From (15) and (23), the constraint is redefined as

$$\boldsymbol{b}^{\mathrm{T}}\boldsymbol{C}(\omega_0, v_k) = 0, k = 1, 2, \ldots, L. \tag{25}$$

If v is a vector of order L, $\boldsymbol{C}$ would be a matrix of order $N \times (L+1)$, where $k = 1$ corresponds to the zeroth-order derivative and equals $B(\omega_0)$.

Equation (25) can be expressed in terms of a matrix as

$$\boldsymbol{C}_x\boldsymbol{b} = \boldsymbol{f} \tag{26}$$

where

$$\boldsymbol{C}_x = \left[\boldsymbol{S}_o(\omega_0) \quad \boldsymbol{C}(\omega_0, v_1) \quad \boldsymbol{C}(\omega_0, v_2)\ldots\boldsymbol{C}(\omega_0, v_{L+1})\right]^{\mathrm{T}} \tag{27}$$

and

$$\boldsymbol{f} = [B(\omega_0) \quad 0 \quad 0\ldots 0]^{\mathrm{T}}. \tag{28}$$

The optimal solution of the objective function defined by (17), with the constraint given by (26), is evaluated using the Lagrange multiplier method [13], and is given as

$$\boldsymbol{b}_{\mathrm{opt}} = \boldsymbol{Q}^{-1}\boldsymbol{P} - \boldsymbol{Q}^{-1}\boldsymbol{C}_x^{\mathrm{T}}\left(\boldsymbol{C}_x\boldsymbol{Q}^{-1}\boldsymbol{C}_x^{\mathrm{T}}\right)^{-1}\left(\boldsymbol{C}_x\boldsymbol{Q}^{-1}\boldsymbol{P} - \boldsymbol{f}\right) \tag{29}$$

which is a closed-form solution, computed very efficiently. The only requirement is to find a suitable order for the FDs and the reference frequency, which can satisfy the constraint. CF-PSO can be used to determine these values.

V. Proposed Method Based on FD and ET

In this section, a new method based on FD and CF-PSO is proposed for the design of a Hilbert transformer using an APF. For analysis, a benchmark design example is considered

This article has been accepted for inclusion in a future issue of this journal. Content is final as presented, with the exception of pagination.

with the design specifications being: order $(N) = 30$, $\omega_1 = 0.04$, and $\omega_2 = 0.94$, using the following attributes:

$$\text{Approximation error: } e_r(\omega) = |\varphi(\omega) - \varphi_d(\omega)| \tag{30}$$

and

$$\text{Total phase error: } E = \int_{\omega_1}^{\omega_2} e_r(\omega) d\omega. \tag{31}$$

A. Proposed Method Based on FD Without ET

For designing a Hilbert transformer using the proposed method, without CF-PSO, initially, the optimal filter coefficients are determined using (29), which requires the optimal value of order (v_3) of FD and the reference frequency point. For this purpose, different values of the reference frequency (ω_0), from ω_1 to ω_2, with a uniform step size of 0.05, are used, while the value of v_3 is considered to vary from 2.01 to 49.99 with a gradual increment of 0.01. Other values of v (v_0, v_1, and v_2) are kept as 0, 1, and 2, respectively, to maintain the slope and concavity of the function [15]. The generalized steps for designing an HT using the proposed method without ET are as follows.

1) Specify the filter parameters, such as N, ω_1, and ω_2, and the desired phase response $\varphi_d(\omega)$.
2) Choose suitable reference frequency points between ω_1 and ω_2, while v_3 varies from 2.01 to 49.99 with a gradual increment of 0.01.
3) Compute $\boldsymbol{S}_o(\omega)$, $\boldsymbol{Q}$, and $\boldsymbol{P}$ using (16), (19), and (20), respectively.
4) Select the reference frequency point and the value of v_3 to compute $\boldsymbol{C}_x$.
5) Evaluate the coefficients of HT using (29), and then, compute E. Store E in a stack for further selection of the optimal values of ω_0 and v_3.
6) Increment v_3 until all the values are utilized. If all the values of v_3 have been used, shift to the next ω_0.

During the experiments, it has been observed that the variation in phase error (E) becomes periodic with a high error value for all ω_0, after a certain value of v_3, as illustrated in Fig. 1(a), because some FDs satisfy the imposed constraints exactly, while others fail to satisfy the required constraint. It is also evident from the experimental results that, at $\omega_0 = 0.74\pi$, 0.85π, and 0.17π, the phase error (E) is less, when v_3 is 6.40, 4.79, and 25.48, respectively. The obtained phase response of a Hilbert transformer is depicted in Fig. 1(b). It can be seen from Fig. 1(c) that the approximation between the desired and designed response is high at the exact value of ω_0.

If the number of FDs is increased, the computational complexity is also increased. The computational complexity for the exploration of one FD along with ω_0 is $o(n^4)$, and it would increase to $o(n^5)$, if two FDs are considered. Thus, the ET-based approach is more effective in such complex evaluation processes through which both the ω_0 and FD values can be adjusted simultaneously with high precision.

B. Proposed Method Based on FD With ET

In this section, the proposed technique for designing an HT is modified further using CF-PSO, owing to its simple

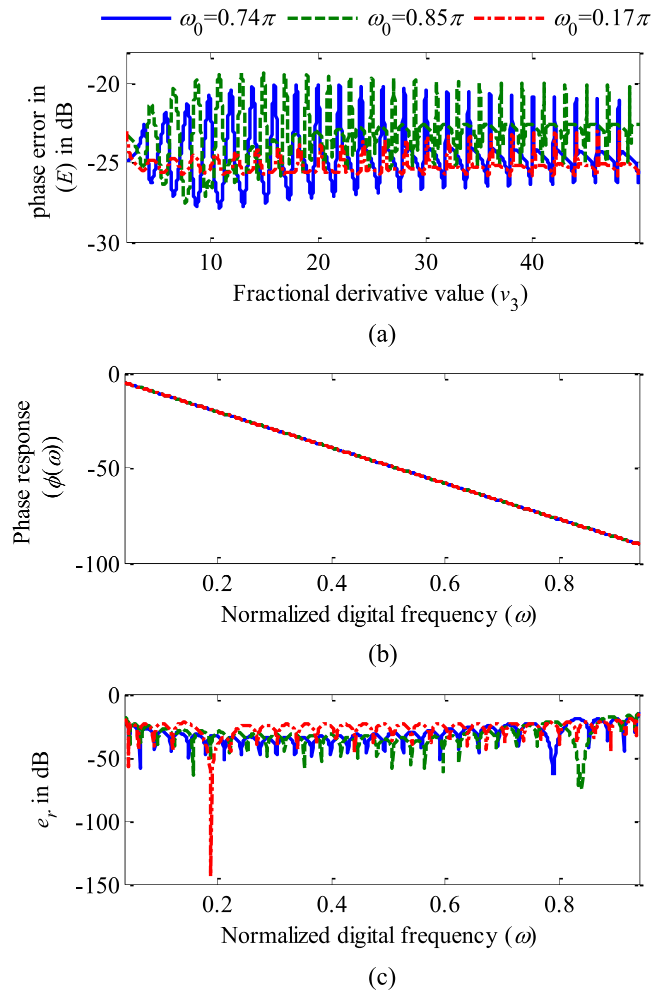

Fig. 1. (a) Variation of phase error with respect to v_3 at three different values of reference frequency (ω_0). (b) Phase response of HT using the first-order FD (1-FD). (c) Variation of absolute error difference of designed HT. Figures show the effect of 1-FD and ω_0 on the performance of the designed HT.

exploration and exploitation mechanism for finding suitable values of FD along with ω_0. The search space ($\boldsymbol{U}$) is formed as

$$[\boldsymbol{U}_{r,t}] = [u_{i,1} \;\; u_{i,2} \;\; u_{i,3} \ldots u_{i,D}] \tag{32}$$

where $1 \le r \le R$ and $1 \le t \le T$, $u_{i,1}$ correspond to the reference frequency points between ω_1 and ω_2, while $u_{i,2}$ to $u_{i,D}$ represent the FD values from 2.01 to 14.99. D is the number of FDs employed. During the course of exploration, if these values have exceeded beyond the imposed limit, they are restored by reassigning suitable values as

$$\boldsymbol{U}_{\text{new}} = \boldsymbol{U}_{\text{low}} \odot \boldsymbol{U}_x + \boldsymbol{U}_{\text{up}} \odot \boldsymbol{U}_x + \{\bar{\boldsymbol{U}}_{\text{low}} \odot \boldsymbol{U} + \bar{\boldsymbol{U}}_{\text{up}} \odot \boldsymbol{U}\} \tag{33}$$

where $\boldsymbol{U}_{\text{low}}$ and $\boldsymbol{U}_{\text{up}}$ are the vectors containing 1s and 0s. In $\boldsymbol{U}_{\text{low}}$, "1s" correspond to the values of $\boldsymbol{U}$ that are below the lower limit value of 2.01 and "0s" correspond to those that are above or equal to 2.01. In $\boldsymbol{U}_{\text{up}}$ 1s represent those values of $\boldsymbol{U}$ that are greater than the upper limit of 14.99 and 0s represent those less than 14.99. $\bar{\boldsymbol{U}}_{\text{low}}$ and $\bar{\boldsymbol{U}}_{\text{up}}$ are the complements of the respective vectors and $\boldsymbol{U}_x$ has new values within the limits.

This article has been accepted for inclusion in a future issue of this journal. Content is final as presented, with the exception of pagination.

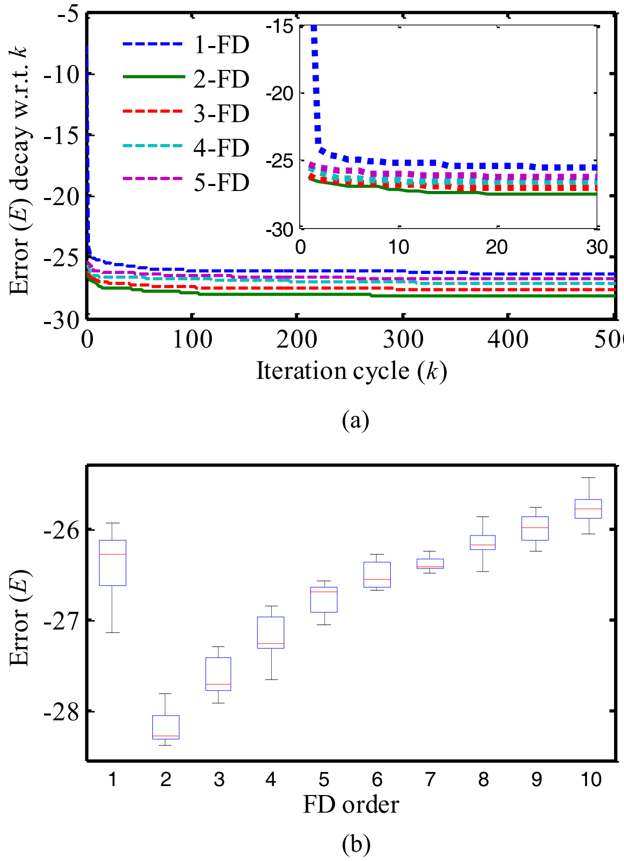

Fig. 2. (a) Mean of convergence of phase error (E) with respect to iteration cycles (k) for FD orders from 1 to 5. (b) Variations in E in each experimental trial for different FD orders ranging from 1 to 10. These figures suggest suitable FD orders and cycles for the proposed method.

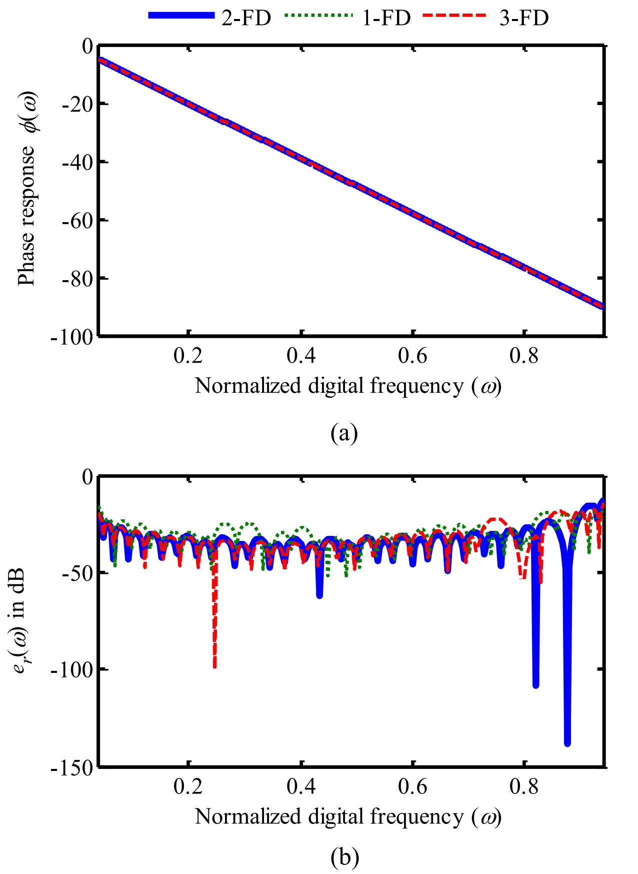

Fig. 3. (a) Hilbert transformer phase response obtained for different filter coefficients using FD: 1, 2, 3. (b) Approximation error. This figure shows that the second-order FD is computationally efficient for designing an HT.

The Hilbert transformer is designed using the same benchmark design specifications as specified in Section V. The fractional order (v) is varied from 1 to 10, and the dimension of matrix $\boldsymbol{C}_x$ is varied from 4 to 14. The control parameter values, such as $\chi = 0.7213$, c_1 and $c_2 = 2.05$, and $w = 1$ are used to control the exploration and exploitation. The normalized digital frequency band is broken into $30 \times N$ equally spaced samples, for analysis. The generalized steps for the proposed method using FD and ET for designing a Hilbert transformer are as follows.

1) Specify the HT parameters, such as N, ω_1, and ω_2, and the desired phase response $\varphi_d(\omega)$.
2) Set the control parameters of CF-PSO, such as χ, c_1, and c_2, and w, maximum iteration count ($k_{\max}$), and upper and lower limits of $\boldsymbol{V}$ and $\boldsymbol{U}$.
3) Formulate the initial search space ($\boldsymbol{U}^{[k=0]}$) and associated velocity ($\boldsymbol{V}^{[k=0]}$) by assigning the uniformly distributed random numbers between the upper and lower limits. Store the initially formed $\boldsymbol{U}$ as ***PB***.
4) Compute the filter coefficients using FD values from each vector of $\boldsymbol{U}$ using (29), followed by the fitness evaluation using (31). Store these fitness values as ***PB fitness***.
5) The solution with the best value of ***PB fitness*** is picked as ***GB,*** and its fitness value is stored in *GB fitness.*
6) Update $\boldsymbol{V}$ using (2), and check for those velocity elements that are not in limit. Then, reassign new values to those outbound elements.
7) Update $\boldsymbol{U}$ using (1) and confirm that all newly formed elements of $\boldsymbol{U}$ are within the bounded limits; otherwise, assign new values for those that are not in the limits.
8) Again, compute the filter coefficients using new FD values, followed by fitness evaluation using (31). Store these fitness values as ***new fitness***.
9) Replace the earlier solutions from ***PB and PB fitness*** with the new solutions that have improved fitness values.
10) Compare the current *GB fitness* with the new ***PB fitness***, and check if any ***PB fitness*** is better than *GB fitness*. If so, replace ***GB*** and *GB fitness* with the improved ***PB*** and ***PB fitness***; else, keep them as they are.
11) Repeat steps 6–10 until the iteration cycle is over or the desired fitness is achieved.

The proposed method is executed 30 times for each FD order. Fig. 2(a) shows the mean convergence of E with respect to the iteration cycles (k) for FD orders from 1 to 5. It is observed that the rate of change of E is almost constant after 30 iterations. Fig. 2(b) indicates that CF-PSO achieves the best performance for the second-order FD, consistently, as the median value of E lies close to the best fitness value achieved during a trial of 30 experiments. The phase responses obtained using first-, second-, and third-order FDs are shown

This article has been accepted for inclusion in a future issue of this journal. Content is final as presented, with the exception of pagination.

Pseudo Code 1 Pseudo Code of Proposed Approach

```
Set N, ω, ω, φ_d(ω), s(ω), c(ω), P, Q, and Q^{-1}
Set χ = 0.707, c_1 = 2.05, c_2 = 2.05, and k_max
Formulate initial search space U
For i = 1 to SS
   Compute C_x for i^th FD vector of U
   Compute b_opt using Q^{-1}, P, and C_x
   Evaluate E and store as PB fitness
   PB_i = U_i
End For
Sort out smallest value of PB fitness
PB Corresponding to smallest PB fitness as GB
Start
   Update V according to variant
   V^{k+1} = χ{w · V^k + c_1^k · φ_1 · (PB^k − U^k) + c_2^k · φ_2 · (GB^k − U^k)}
   Restore out of bound elements of V
   Update U as U^{k+1} = U^k + V^{k+1}
   Restore out of bound elements of U
   For i = 1 to SS
      Compute C_x for i^th FD vector of U^{k+1}
      Compute b_opt using Q^{-1}, P, and C_x
      Evaluate E and store as Enew
      If E_new(U_i^{k+1}) < E(PB fitness_i^k)
         PB fitness_i^{k+1} = E_new(U_i^{k+1}) & PB_i^{k+1} = U_i^{k+1}
         If PB fitness_i^{k+1} < E(GB)
            GB = PB_i^{k+1}
         End If
      End If
   End For
End
GB holds best fractional values
```

in Fig. 3(a), while Fig. 3(b) displays the approximation error ($e_r(\omega)$) obtained during the design of a Hilbert transformer. It is evident from the experimental results that the approximation error is comparatively less for 2-FD, while it is high for the first- and third-order FD cases. CF-PSO explores the optimal value of ω_0, and restricts E to remain as low as possible. Therefore, after exhaustive analysis, it is established that the second-order FD explored by CF-PSO is a computationally efficient methodology for designing a Hilbert transformer using APF. The complete design procedure is summarized in Pseudocode 1.

VI. Results and Discussion

All the experiments were performed using MATLAB 2014 on a Genuine Intel CPU i7 3770 @ 3.40 GHz with 4 GB RAM. The following fidelity parameters were computed as:

$$e_{ph}^{\max} = \max_{\omega\in[\omega_1,\omega_2]} |\varphi_d(\omega) - \varphi(\omega)| \tag{34}$$

$$e_{ph}^{\text{tol}} = \sum |\varphi_d(\omega) - \varphi(\omega)|^2 \tag{35}$$

$$e_{\tau}^{\max} = \max_{\omega\in[\omega_1,\omega_2]} \left| \frac{d\varphi_d(\omega)}{d\omega} - \frac{d\varphi(\omega)}{d\omega} \right| \tag{36}$$

and

$$e_{\tau}^{\text{tol}} = \sum \left(\left| \frac{d\varphi_d(\omega)}{d\omega} - \frac{d\varphi(\omega)}{d\omega} \right| \right)^2 \tag{37}$$

TABLE I
Control Parameters for Variants of PSO and Hybrid PSO

	Parameter	Value
Common parameters for all variants of PSO	Constraint factor (χ)	1
	Cognitive coefficient (c_1)	2.05
	Social coefficient (c_2)	2.05
	Upper limit of $\boldsymbol{U}$	14.99
	Lower limit of $\boldsymbol{U}$	2.01
	Upper limit of $\boldsymbol{V}$	14.99
	Lower limit of $\boldsymbol{V}$	-14.99
	Maximum number of cycles	500
CWI-PSO	w	0.700
CF-PSO	w	1.000
	χ	0.707
LDI-PSO	$w_{\min}$	0.7
	$w_{\max}$	0.1
NDI-PSO	Modulation index (η)	0.2 to 1.4
TVC-PSO	$c_1^{initial}$, c_2^{final}	2.05
	c_1^{final}, $c_2^{initial}$	0.05
Hybrid-PSO	*limit*	30

TABLE II
Statistical Performance Evaluation of Proposed Technique for an SS of 10

N		$e_{ph}^{\max}$	e_{ph}^{tol}	$e_{\tau}^{\max}$	e_{τ}^{tol}	Time (sec)
15	best	0.3443	0.5947	4.9791	223.3440	20.4531
	mean	0.3699	0.6981	5.0642	230.4314	23.4219
	worst	0.4296	0.9674	5.0910	235.2774	25.1563
20	best	0.1782	0.1208	4.5578	105.7094	23.1094
	mean	0.1905	0.1414	4.6412	113.2186	24.7625
	worst	0.2101	0.1737	4.7582	124.1955	26.1406
25	best	0.0850	0.0220	3.4221	36.4655	24.6719
	mean	0.0915	0.0257	3.5289	39.9048	26.0000
	worst	0.1095	0.0362	3.8054	48.8362	28.9531
30	best	0.0370	0.0038	2.1743	11.0042	31.3906
	mean	0.0416	0.0047	2.3265	12.7637	31.8719
	worst	0.0482	0.0061	2.5347	15.4151	32.4844
35	best	0.0145	0.0005	1.1749	2.4623	36.8906
	mean	0.0162	0.0007	1.2660	2.8768	37.7719
	worst	0.0180	0.0008	1.3609	3.3389	38.4063
40	best	0.0065	0.0001	0.6529	0.6862	53.2031
	mean	0.0069	0.0001	0.6844	0.7505	53.8031
	worst	0.0079	0.0002	0.7570	0.9032	54.4531
50	best	0.0009	0.0000	0.1381	0.0292	64.4531
	mean	0.0011	0.0000	0.1521	0.0343	66.1750
	worst	0.0011	0.0000	0.1629	0.0384	67.0313

where $e_{ph}^{\max}$ is the maximum phase error (MPE), e_{ph}^{tol} is the total squared phase error (TSPE), $e_{\tau}^{\max}$ is the maximum group delay error (MGDE), and e_{τ}^{tol} is the total group delay error (TGDE), used for analyzing the proficiency of the proposed method.

A. Design Examples Using Proposed Methodology

In the proposed method, different variants of PSO, such as the constant weight inertia PSO (CWI-PSO), linearly decaying inertia PSO (LDI-PSO), NDI-PSO, dynamic inertia PSO (DI-PSO), and time-varying coefficients PSO (TVC-PSO) were exploited for finding the appropriate values of FDCs. After exhaustive experimental analysis, suitable variant of PSO is selected in the proposed approach of HT using FDC. PSO is classified based on the updating strategy of the principle (2), and more details are presented in [16]. Recently,

This article has been accepted for inclusion in a future issue of this journal. Content is final as presented, with the exception of pagination.

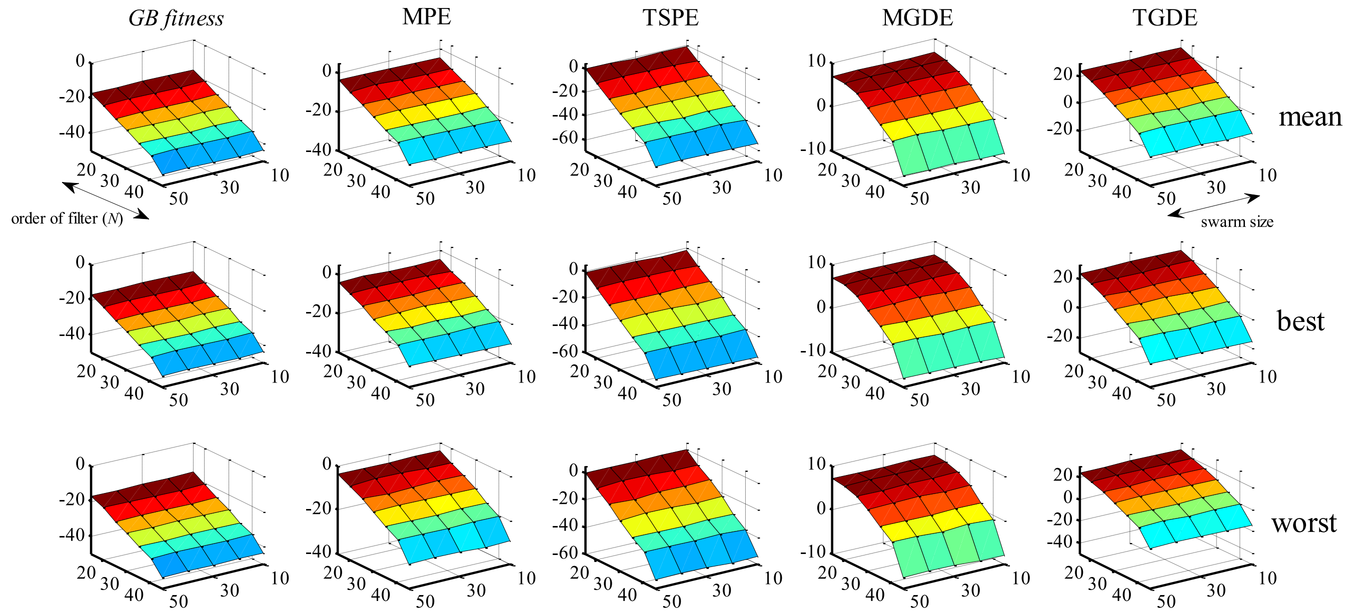

Fig. 4. Statistical performance evaluation of proposed technique for different filter orders, designed by different SS on the basis of global best fitness (*GB fitness*), MPE, TSPE, MGDE, and TGDE. The first row of the plot shows the mean of output obtained after 30 trials, second row shows the best, and third row shows the worst output values for all five parameters. The stability of the proposed method is consolidated in these figures.

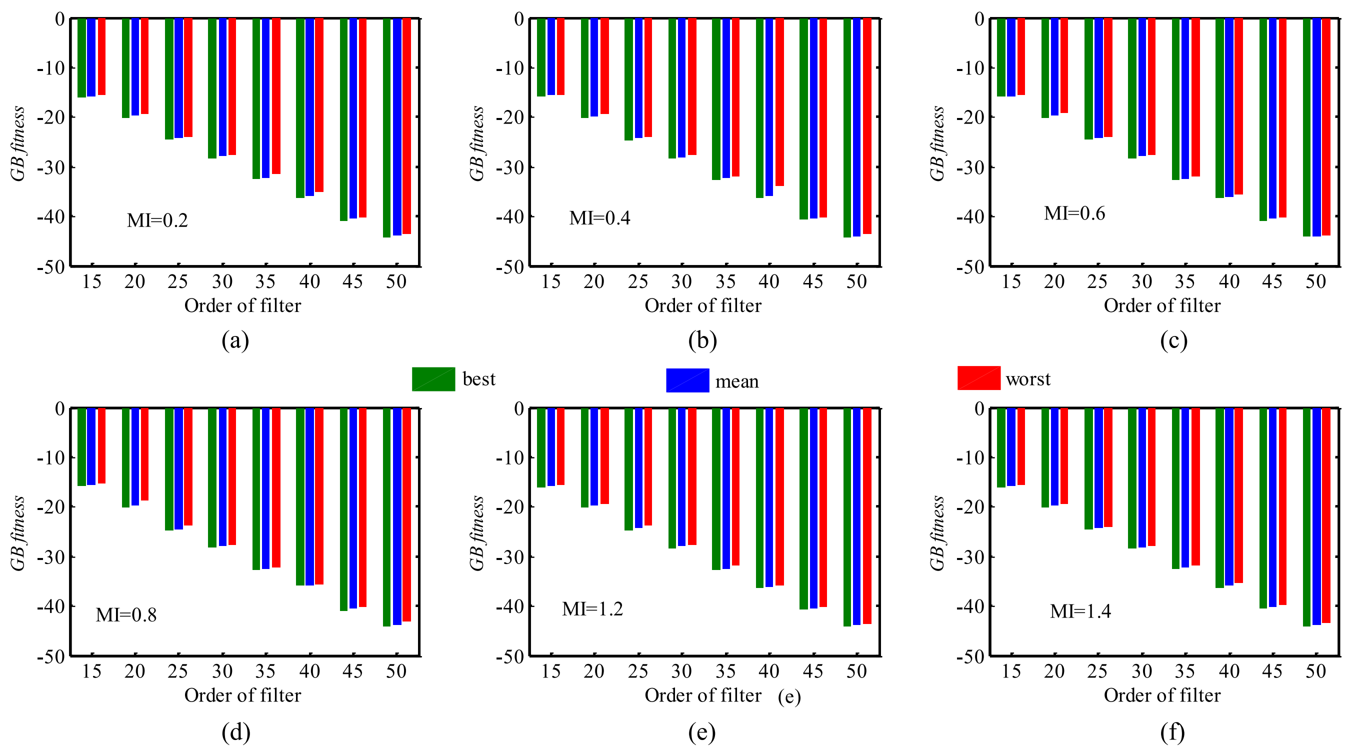

Fig. 5. Statistical performance evaluation of nonlinearly decaying inertia PSO (NDI-PSO) based on mean, best, and worst values of *GB fitness* (dB) for design of HTs of various orders using different values of MI. (a) MI = 0.2, (b) MI = 0.4, (c) MI = 0.6, (d) MI = 0.8, (e) MI = 1.2, and (f) MI = 1.4. There is a marginal deviation on GB fitness value for different values of MI.

hybrid-PSO based on the combined functionality of PSO and ABC algorithms was proposed in [22]. It is also used in this paper. The control parameters of all the variants of PSO, including hybrid-PSO, are summarized in Table I. For comparison, a design example from [4] and [7] was considered, with a normalized frequency band from 0.04 to 0.94 and filter order from 15 to 50, with an increment of 5. The effect of swarm size (SS) was analyzed by varying it from 10 to 50 for each design case. It is evident from Fig. 4 that, for all filter orders considered in this paper, the SS of 10 is sufficient as the deviations of the best and worst of the fidelity parameters, from the mean values, are less. The detailed simulation analysis for an SS of 10 is summarized in Table II.

This article has been accepted for inclusion in a future issue of this journal. Content is final as presented, with the exception of pagination.

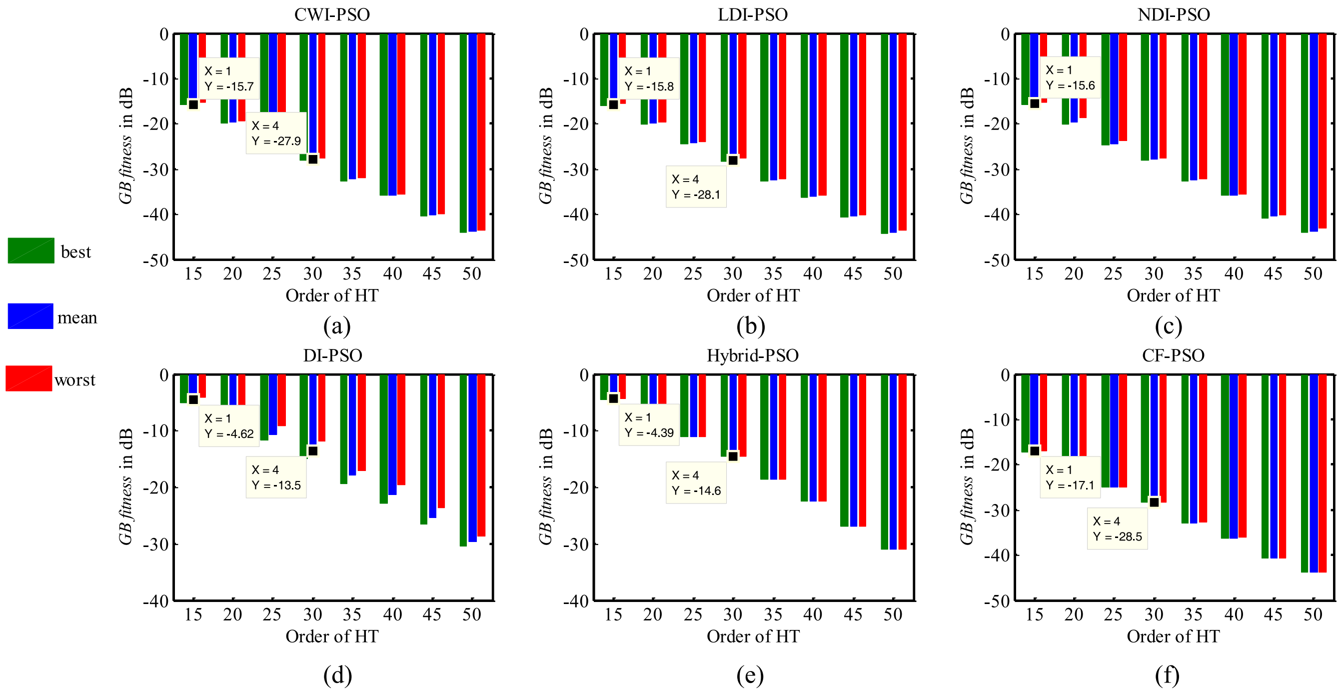

Fig. 6. Comparative evaluations of PSO variant based on best, mean, and worst values of *GB fitness* obtained for the design of HTs with various orders. (a) CWI-PSO, (b) LDI-PSO, (c) NDI-PSO, (d) DI-PSO, (e) Hybrid-PSO, (f) CF-PSO. It is confirmed that the proposed method works effectively when CF-PSO is used.

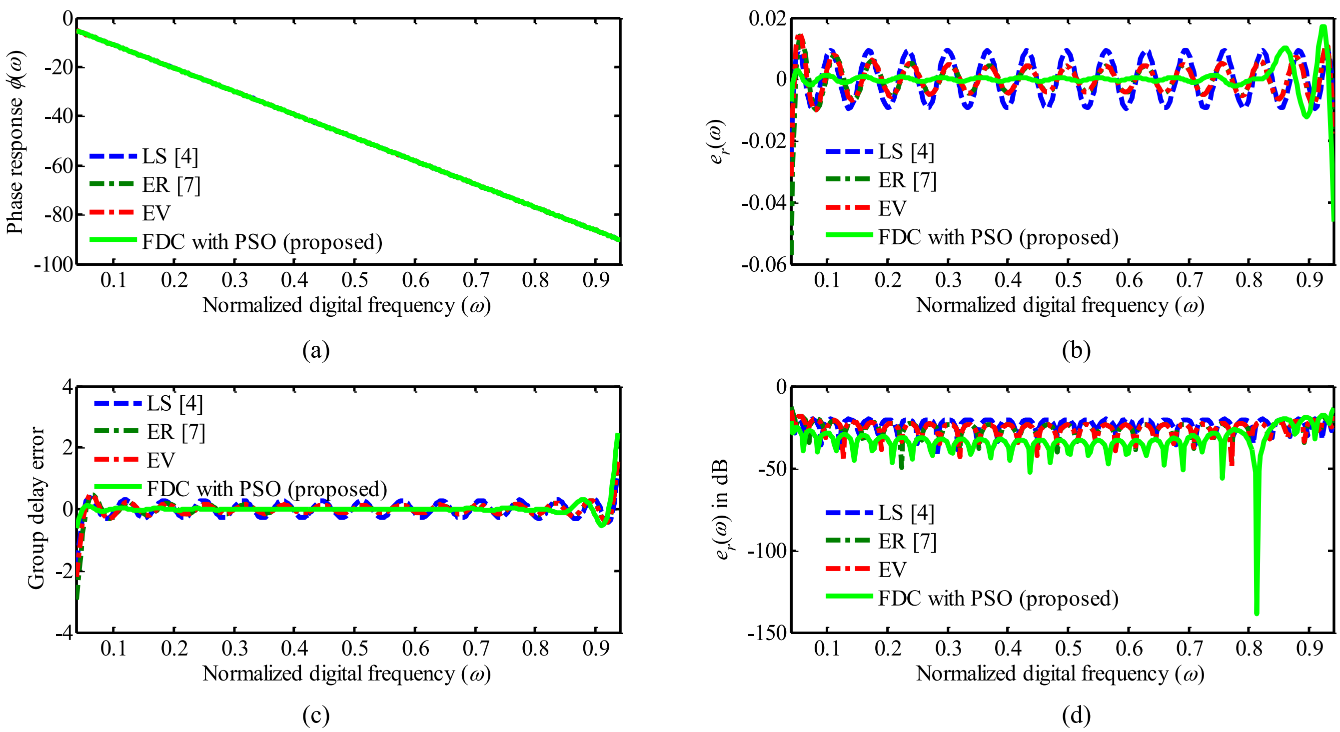

Fig. 7. (a) Phase response of Hilbert transformer, (b) approximation error, (c) group delay error, (d) approximation error in dB for LS, ER, EV, and proposed method (FD with PSO). FD-based design approach resulted in flat group delay response and significant reduction in $e_T(\omega)$.

On the basis of an exhaustive analysis performed using CF-PSO, it was confirmed that the SS of 10 was a reasonable choice that required less computation time. Therefore, an SS = 10 was used for all variants of PSO and hybrid-PSO, for further analysis. In NDI-PSO, the modulation index (MI) value was used to control w and its value had to be determined experimentally. Therefore, exhaustive experiments were conducted using different values of MI, ranging from 0.2 to 1.4 with an increment of 0.2, excluding 1.0 because it corresponded to LDI-PSO. The obtained results are consolidated in Fig. 5,

This article has been accepted for inclusion in a future issue of this journal. Content is final as presented, with the exception of pagination.

TABLE III
COMPARISON WITH OTHER METHODS [4], [7]

Technique	N	e_{ph}^{max}	e_{ph}^{tol}	e_{τ}^{max}	e_{τ}^{tol}
LS [4]	30	2.927×10^{-2}	6.787×10^{-3}	2.4962	22.0373
ER [7]	30	9.550×10^{-3}	1.325×10^{-2}	1.325	19.5756
EV	30	3.157×10^{-2}	7.155×10^{-3}	2.1847	17.1662
Proposed	30	4.619×10^{-2}	5.618×10^{-3}	2.4761	14.5328

which shows the statistical performances of the different values of MI, in terms of the quality of solution. It was confirmed that, in the case of the proposed method, NDI-PSO had almost similar performance and MI $= 0.8$, which had marginal advantage over the other values. Thus, MI $= 0.8$ was chosen for further comparative analysis. HTs with different orders were designed using different variants of PSO and Hybrid PSO and their comparative performances, on the basis of *GB fitness,* is shown in Fig. 6. It is evident from Fig. 6 that, for lower-order HTs, the proposed method using CF-PSO yields better performance when compared to other variants of PSO. It is also observed that, for each design, the objective function's mean and worst values are close to the best value.

B. Comparison With Previous State-of-the-Art Methods

For comparison, a Hilbert transformer was designed using the proposed method based on FD and ET using $N = 30$, $\omega_1 = 0.04$, and $\omega_2 = 0.94$ [4], [7]. In this case, an SS of 10, with 50 iterations were used. The experimental results obtained using the proposed method are illustrated in Fig. 7, along with the results of methods, such as the LSs, equiripple (ER), and EV. It was observed that the value of e_{ph}^{tol} was 5.618×10^{-3} when using the proposed method, and it was 6.787×10^{-2} and 1.325×10^{-2} for the LS technique and ER technique, respectively. However, $e_{ph}^{\max}$ was increased slightly to 4.619×10^{-2} for the proposed method, while it was 2.927×10^{-2} and 9.550×10^{-3} in the case of LS and ER, respectively. The value of $e_r(\omega)$ was less, up to ω_0, and was increased slightly afterward, as shown in Fig. 7(b) and (d). Meanwhile, the values of $e_{ph}^{\max}$ and $e_{\tau}^{\max}$ were reduced, when compared to those of other techniques. Therefore, it was confirmed that the reference frequency point had been selected appropriately, which resulted in a reduction in the overall phase error. The performance of the designed APF-based HT, using the proposed methodology, is summarized in Table III. There is a reduction of 57% in total phase error (e_{ph}^{tol}) when compared with LS and ER techniques.

VII. CONCLUSION

This paper presented a new design method for HTs using an APF, based on FDs and CF-PSO. The optimal values of the FDs and the reference frequency point, for obtaining improved performance, were determined using CF-PSO. The experimental results illustrated the superiority of the proposed algorithm in terms of phase response and reduction of overall error, in comparison with the other existing techniques. In the future, the proposed method can be extended to compute FDs at more reference frequency points so that the other fidelity parameters may also be reduced with high degrees of approximation. There is a slight rise in $e_{ph}^{\max}$and may be controlled by forming multiobjective optimization problem. The presented work may be extended for efficient realization using canonic signed digit.

REFERENCES

[1] Y. Liu, *Hilbert Transform and Applications*, InTech, London, U.K., 2012.
[2] D. Helbing *et al.*, "Saving human lives: What complexity science and information systems can contribute," *J. Stat. Phys.*, vol. 158, no. 3, pp. 735–781, Feb. 2015.
[3] Q. Wu *et al.*, "Classification of EMG signals by BFA-optimized GSVCM for diagnosis of fatigue status," *IEEE Trans. Autom. Sci. Eng.*, vol. 14, no. 2, pp. 915–930, Apr. 2017.
[4] Y.-D. Jou, Z.-P. Lin, and F.-K. Chen, "Low-complexity design framework of all-pass filters with application in quadrature mirror filter banks design," *IET Signal Process.*, vol. 11, no. 3, pp. 239–249, May 2017.
[5] T. Q. Nguyen, T. I. Laakso, and R. D. Koilpillai, "Eigenfilter approach for the design of allpass filters approximating a given phase response," *IEEE Trans. Signal Process.*, vol. 42, no. 9, pp. 2257–2263, Sep. 1994.
[6] A. Djebbari, J. M. Rouvaen, A. Djebbari, M. F. Belbachir, and S. A. Elahmar, "A new approach to the design of limit cycle-free IIR digital filters using eigenfilter method," *Signal Process.*, vol. 72, no. 3, pp. 193–198, Feb. 1999.
[7] S. S. Kidambi, "Weighted least-squares design of recursive allpass filters," *IEEE Trans. Signal Process.*, vol. 44, no. 6, pp. 1553–1557, Jun. 1996.
[8] G. Stančić and S. Nikolić, "Digital linear phase notch filter design based on IIR all-pass filter application," *Digital Signal Process.*, vol. 23, no. 3, pp. 1065–1069, May 2013.
[9] L.-C. Su, Y.-D. Jou, and F.-K. Chen, "Improved computing-efficiency least-squares algorithm with application to all-pass filter design," *Math. Problems Eng.*, vol. 2013, pp. 1–8, May 2013.
[10] D. Idiou, A. Charef, and A. Djouambi, "Linear fractional order system identification using adjustable fractional order differentiator," *IET Signal Process.*, vol. 8, no. 4, pp. 398–409, Jun. 2014.
[11] J. Bai and X.-C. Feng, "Fractional-order anisotropic diffusion for image denoising," *IEEE Trans. Image Process.*, vol. 16, no. 10, pp. 2492–2502, Oct. 2007.
[12] Y. Ferdi, J. P. Herbeuval, A. Charef, and B. Boucheham, "R wave detection using fractional digital differentiation," *ITBM-RBM*, vol. 24, nos. 5–6, pp. 273–280, 2003.
[13] C.-C. Tseng and S.-L. Lee, "Design of linear phase FIR filters using fractional derivative constraints," *Signal Process.*, vol. 92, no. 5, pp. 1317–1327, May 2012.
[14] C. C. Tseng and S. L. Lee, "Fractional derivative constrained design of FIR filter with prescribed magnitude and phase responses," in *Proc. Eur. Conf. Circuit Theory Design (ECCTD)*, 2013, pp. 1–4.
[15] K. Baderia, A. Kumar, and G. K. Singh, "Hybrid method for designing digital FIR filters based on fractional derivative constraints," *ISA Trans.*, vol. 58, pp. 493–508, Sep. 2015.
[16] M. K. Ahirwal, A. Kumar, and G. K. Singh, "EEG/ERP adaptive noise canceller design with controlled search space (CSS) approach in Cuckoo and other optimization algorithms," *IEEE/ACM Trans. Comput. Biol. Bioinf.*, vol. 10, no. 6, pp. 1491–1504, Nov./Dec. 2013.
[17] J. Zhang, C. Zhang, T. Chu, and M. Perc, "Resolution of the stochastic strategy spatial Prisoner's dilemma by means of particle swarm optimization," *PLoS ONE*, vol. 6, no. 7, Jul. 2011, Art. no. e21787.
[18] I. Fister *et al.*, "Particle swarm optimization for automatic creation of complex graphic characters," *Chaos Solitons Fractals*, vol. 73, pp. 29–35, Apr. 2015.
[19] F. Li and J. Guo, "Topology optimization of particle swarm optimization," in *Advances in Swarm Intelligence. ICSI* (Lecture Notes in Computer Science), Y. Tan, Y. Shi, and C. A. C. Coello, Eds. Cham, Switzerland: Springer, 2014, pp. 142–149.
[20] M. Yang, Z. Cai, C. Li, and J. Guan, "An improved JADE algorithm for global optimization," in *Proc. IEEE Congr. Evol. Comput. (CEC)*, 2014, pp. 806–812.
[21] T. Ni, L. Wang, Q. Jiang, J. Zhao, and Z. Zhao, "LSHADE with semi-parameter adaptation for chaotic time series prediction," in *Proc. 10th Int. Conf. Adv. Comput. Intell. (ICACI)*, 2018, pp. 741–745.

This article has been accepted for inclusion in a future issue of this journal. Content is final as presented, with the exception of pagination.

[22] S. M. Rafi, A. Kumar, and G. K. Singh, "An improved particle swarm optimization method for multirate filter bank design," *J. Franklin Inst.*, vol. 350, no. 4, pp. 757–769, May 2013.

Anil Kumar (M'16) received the B.E. degree in electronic and telecommunication engineering from the Army Institute of Technology, Pune University, Pune, India, in 2002 and the M.Tech. and Ph.D. degrees in electronic and telecommunication engineering from IIT Roorkee, Roorkee, India, in 2006 and 2010, respectively.

He is an Assistant Professor with the Electronic and Communication Engineering Department, Indian Institute of Information Technology, Design and Manufacturing, Jabalpur, India. He is currently a Visiting Researcher with the Gwangju Institute of Science and Technology, Gwangju, South Korea. His current research interests include the design of digital filters and filterbanks, biomedical signal processing, image processing, and speech processing.

Nikhil Agrawal (S'15) received the bachelor's degree in electronics and communication engineering from Rajiv Gandhi Proudyogiki Vishwavidyalaya, Bhopal, India, in 2010. He is currently pursuing the Ph.D. degree in electronics and communication engineering, PDPM Indian Institute of Information Technology, Design and Manufacturing Jabalpur, Jabalpur, India.

His current research interests include designing optimal filters, optimization techniques, and embedded system design for signal processing.

Ila Sharma (S'17) received the Ph.D. degree in electronic and communication engineering from the PDPM Indian Institute of Information Technology Design and Manufacturing Jabalpur, Jabalpur, India.

Her current research interests include multirate filterbanks, digital signal processing, multiplierless filters and filterbanks, wireless communication, and cognitive radio. She has been engaged in active research work and a novel approach to the above fields. She has published/presented a number of research articles in various journals and conferences in the above areas.

Seungchan Lee received the B.S. degree in electronic engineering from Chungbuk National University, Cheongju, South Korea, in 2009 and the M.S. degree in electrical engineering and computer science from the Gwangju Institute of Science and Technology, Gwangju, South Korea, in 2012, where he is currently pursuing the Ph.D. degree in biomedical signal processing.

His current research interests include machine learning, biomedical signal processing, adaptive signal processing, brain computer interface, and the design of wearable EEG/fNIRS hybrid brain monitoring systems.

Heung-No Lee (SM'93) received the B.S., M.S., and Ph.D. degrees in electrical engineering from the University of California at Los Angeles, Los Angeles, CA, USA, in 1993, 1994, and 1999, respectively.

He was a Research Staff Member with HRL Laboratory, Malibu, CA, USA, from 1999 to 2002. He was then appointed as an Assistant Professor with the University of Pittsburgh, Pittsburgh, PA, USA, in 2002. In 2009, he joined the Gwangju Institute of Science and Technology (GIST), Gwangju, South Korea, as an Associate Professor, where he was promoted to a Full Professor in 2013. He was the Director of electrical engineering and computer science track with GIST in 2014, where he was appointed the Dean of Research in 2015. He has published over 40 international journal publications and 100 international conferences and workshop papers. His current research interests include information theory, signal processing theory, and communications theory, and the application to wireless communications and networking systems, compressive sensing and optical engineering, biomedical systems, and brain computer interfaces.

Dr. Lee was a recipient of the Top 50 Research and Development Achievements of Fundamental Research in 2013 (National Research Foundation), the Top 100 National Research and Development Research Award in 2012 (the Ministry of Science, ICT and Future Planning), and This Month Scientist/Engineer Award (National Research Foundation) in 2014. He has served as the Lead Guest Editor for the *EURASIP Journal on Wireless Communications and Networking* in 2010 and 2011, and has been an Area Editor for the *AEU International Journal of Electronics and Communications* since 2013. He was the Chapter Chair for the IEEE Signal Processing Society with Pittsburgh, from 2005 to 2008. He has served as Secretary of the IEEE Gwangju Section in Gwangju, from 2010 to 2011. He has been the Chair of the IEEE Gwangju Section since 2012. He has served as a member of technical program committees for IEEE conferences, including the IEEE International Conference on Communications and IEEE Globecom.